Synthesis and Separation of *meso*-erythritol Oligomers as Isoprene-Derived Secondary Organic Aerosol Surrogates

Benjamin Fawcett

Senior Honors Thesis
Department of Chemistry
The University of North Carolina at Chapel Hill

April 4, 2019

Approved:

_____

Dr. Avram Gold, Thesis Advisor

Dr. Erik Alexanian, Reader

Dr. Paul Kropp, Reader

Abstract:

Isoprene-derived secondary organic aerosols are produced *en masse* in regions with high density of deciduous flora. These compounds produce fine aerosol particles that have been suggested to pose significant cardiovascular health risk. Oligomers comprised of C_5 units contribute significantly to aerosol content. To date, there is no available standard for quantitation of these compounds, which can make up over 40% of the fine organic aerosol mass during seasonal fluctuations.[1] Structural cognates have been synthesized to remediate this obstacle, with substantial efforts to isolate and purify these compounds to be used as standards for estimating the oligomeric content in atmospheric field samples. With isolated compounds, molecular characterization via ^{1}H and ^{13}C NMR can be performed, to confirm the identity of these compounds. Availability of these compounds as standards would open new opportunities for studies to quantify the flux of these atmospheric particles, as well as to further elucidate cellular responses to exposure.

Introduction:

The two most abundant biogenic volatile organic compounds (VOCs) emitted into the global atmosphere are isoprene and methane.[2] As with other VOCs, gaseous isoprene (2-methyl-1,3-butadiene, C_5H_8) reacts with hydroxyl radicals and forms less volatile secondary organic aerosol (SOA) via condensation or uptake onto particulates through cascading oxidative pathways.[3] In the United States, isoprene is emitted most heavily in the southeast due to the high density of deciduous forests, and during the summer it is the predominant biogenic VOC released into the atmosphere.[2,4] SOAs have been identified as contributors to fine atmospheric particulate matter (particles with diameter less than 2.5 μm - $PM_{2.5}$). During peak isoprene emission in the southeastern U.S., isoprene-derived SOA can make up 40% of the organic mass of $PM_{2.5}$.[1] Because of the significant role $PM_{2.5}$ plays in the scattering of solar and terrestrial radiation, isoprene-derived SOA may have implications for global climate.[5] $PM_{2.5}$ has also been found to cause serious adverse cardiovascular outcomes, decreased lung function and overall increased risk for mortality, making isoprene-derived SOA not only an environmental concern, but also a public health concern.[6]

Background:

Of particular interest are the dimer polyol aerosol phase compounds derived from IEPOX (Figure 1). Atmospheric chemists have been able to qualitatively detect these compounds in field samples, but have not been able to precisely quantify their presence, as there is currently no commercially available standard to use as a reference. With an available synthetic pathway for formation of such a reference standard, improved geospatial quantification of these compounds can be obtained. With improved measurement, correlative studies can be performed to understand more about the risks of isoprene-derived aerosols to environmental and human health. Additionally, further application of this principle can be applied to designing synthetic schemes for similar aerosol compounds, with emphasis on further derivatives of the isoprene SOA.

Figure 1 illustrates gas-phase oxidative pathways to isoprene SOA precursors, and subsequent pathways leading to SOA. The aerosol phase products of interest for this project are the 10 carbon (C_{10}) dimers, whose structure is highlighted in yellow in Figure 1, that are believe to make up the bulk of isoprene SOA mass.[7] Using *meso*-erythritol as an inexpensive surrogate for the monomeric aerosol precursor species 2-methylerythritol (2ME), I synthesized isomeric dimers through dehydrative etherization, and confirmed their presence with GC/MS analysis after trimethyl silyl derivatization (Figure 2). The products are structural cognates of the isoprene-derived dimers highlighted in Figure 1, differing in the absence of the methyl group.

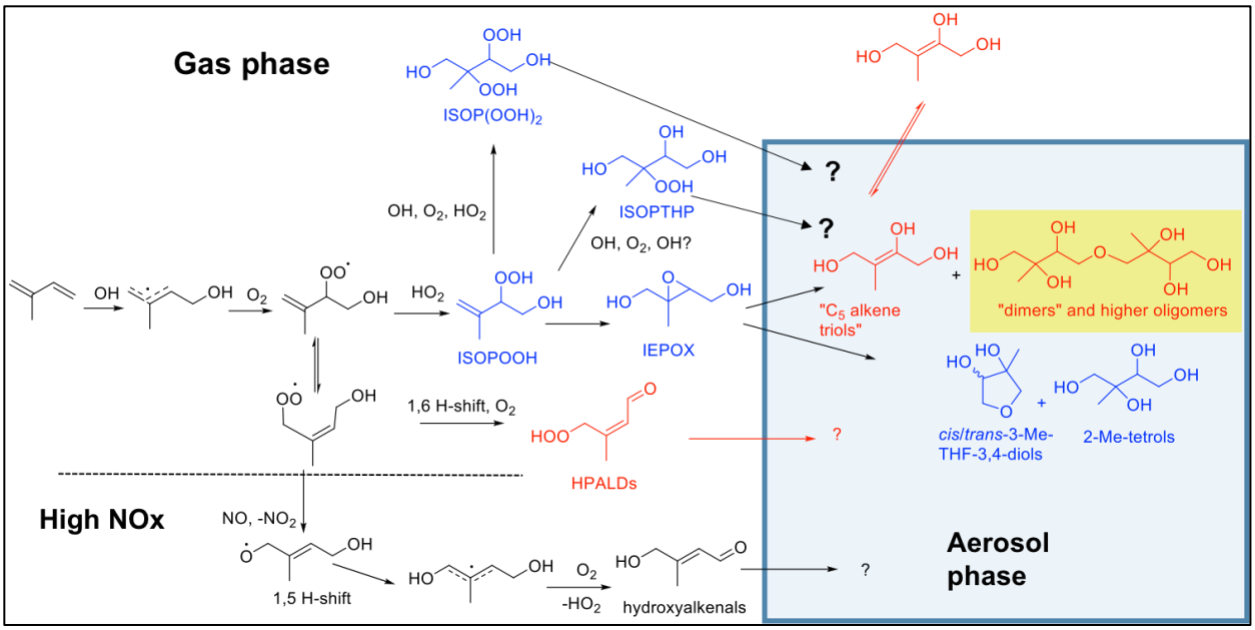

Figure 1: Known isoprene oxidation mechanisms yielding isoprene-derived SOA. Blue species correspond to SOA precursors that we have synthesized in our laboratory. Red species correspond to synthetic targets for future work that will increase our understanding of the isoprene oxidation mechanism yielding SOA. The SOA dimers that are the focus of this work are highlighted in yellow.

Impact:

Meso-erythritol derived dimers, either as completely resolved isomers or as mixtures, can serve as surrogate standards for more accurate quantification of oligomeric components in SOA from field samples in isoprene-rich regions. Quantitation of C_{10} and higher oligomers shown in Figure 1 has to date eluded atmospheric chemists. Furthermore, the synthetic method can be adjusted to generate oligomers of increased chain length, to further enhance quantitative analysis of atmospheric isoprene SOA, and can also be modified to produce robust standards for detection. Availability of individual compounds or well-characterized mixtures of major SOA components will improve air quality models and investigations into the effects of SOA on air quality and climate.

A further application of available pure dimers or well-characterized mixtures derived from 2ME will be the capability to study the effects of major SOA components on human health, both at the cellular level and through correlation of SOA levels with epidemiologic studies. It is already known that $PM_{2.5}$ has adverse effects on cardiovascular health, but a more focused study on the cellular mechanisms of isoprene SOA will provide insight into risks for people living in areas with high isoprene emissions, such as the southeastern U.S.

Materials and Methods:

Dimerization Reaction:

The dimerization reaction was based on studies reported for the dehydration of glycerol to low molecular weight polyhydroxylated oligomeric ethers.[8] Neat *meso*-erythritol mixed with a catalytic quantity of Na_2CO_3 (2% by weight rel. to *meso*-erythritol) was

heated under inert conditions (low flow Argon gas) for 17 hours at 200 – 210ºC in an oil bath.

Derivatization Conditions:

Derivatization with tert-butyldiphenylsilyl chloride (TBDPSCl) was carried out under inert conditions in dry pyridine, with 1g of crude dimer product mixed with 2.5 equivalents of TBDPSCl relative to the monomeric erythritol weight of the product used. A catalytic quantity of 4-dimethylaminopyridine was also included. The reaction mixture was heated at 60ºC for 1 hour, and the pyridine was removed through an azeotropic distillation with toluene, followed by a liquid-liquid extraction with chloroform and an aqueous solution of $CuSO_4$ to completely remove pyridine from the product.

GC/EI-MS:

GC/EI-MS was used as previously described after prior derivatization with trimethylsilane (TMS).[9]

LC/MS (HILIC):[10]

An Agilent 1200 HPLC system coupled with an Agilent 6520 Accurate Mass Q-TOF mass spectrometer with electrospray ionization (ESI) operating in negative ion mode was used with a Waters UPLC BEH Amide column (2.1 × 150 mm, 1.7 µm particle) at 26 ºC. Mobile phases A: 0.1% ammonium acetate in water and B: 0.1% ammonium acetate in 95% acetonitrile, 5% water were used for separation, with each adjusted to a pH of 9.0 with NH_4OH to aid in ionization. The protocol, as outline by Cui, et al., was run over the course of 30 minutes, starting with 100% eluent B for the first 4 minutes, decreasing to 85% over minutes 4-20, held constant from minutes 20-24, increasing back to 100% from minutes 24-25, and remaining constant until the end of the run.[10] The flow rate was 0.300 mL/min throughout the entire method, with 5 µL injection volumes. The mass spectrometer resolved values of *m/z* from 50 to 1000.

LC/MS (Fluoro-Phenyl):

A Waters Acquity UPLC system coupled with a ThermoFisher Quantum Ultra triple-quadrupole mass spectrometer with atmospheric pressure chemical ionization (APCI) operating in negative ion mode was used with an Acquity UPLC CSH Fluoro-Phenyl column (2.1 mm × 100 mm, 1.7 µm particles). Mobile phases A: 10 mM ammonium acetate in water and B: methanol were used for separation. An isocratic method was used with a flow rate of 0.300 mL/min over 7 minutes, with 5 µL injection volumes. The mass spectrometer resolved values of *m/z* from 500 to 900.

^{1}H-NMR:

^{1}H-NMR spectra were acquired at 400 MHz on an Inova 400 MHz spectrometer. Samples were prepared in $CDCl_3$.

^{13}C-NMR:

^{13}C-NMR spectra were acquired at 125 MHz on an Inova 400 MHz spectrometer. Samples were prepared in $CDCl_3$.

Results:

After carrying out the dimerization reaction of *meso*-erythritol and derivatizing the reaction product with trimethyl silyl groups to facilitate volatilization, GC/EI-MS was used to confirm and quantify the dimeric product formation following a published procedure.[9] Figure 2 shows the monomeric peak corresponding to erythritol labelled (0), as well as 3 later retention peaks that are indicative of dimer formation labelled (1), (2), (3). Peaks 1, 2, and 3 have retention times corresponding to detected dimeric compounds previously reported by Surratt, et. al.[9] The reaction conditions yielded approximately 50% conversion from monomer to dimer.

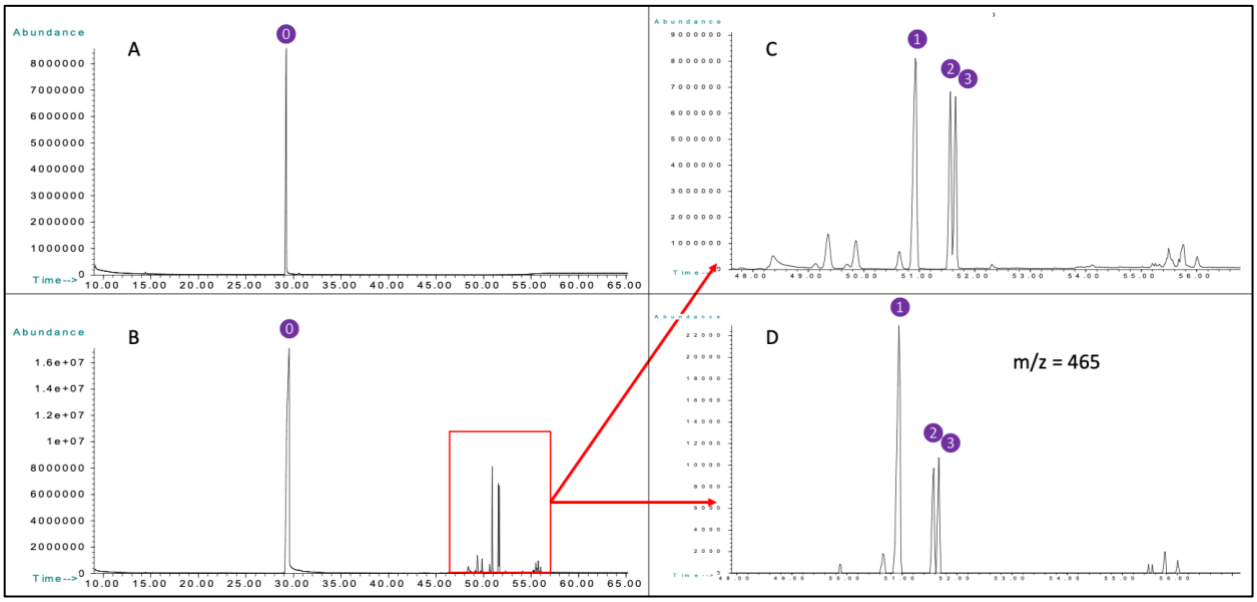

Figure 2: (A): GC/EI-MS trace for erythritol (300 ppm) control. (B): GC/EI-MS trace for 17 hr reaction mixture. (C): GC/EI-MS trace from B, 48-57 mins. (D): Extracted Ion Chromatogram (EIC) for timeframe shown in C for *m/z* = 465.

The presence of dimeric compounds was also confirmed via ^{13}C NMR spectroscopy, with characteristic peaks in the 75-70 ppm region that have been previously confirmed as the range in which the dimeric backbone carbons are observed in Figure 3.[11]

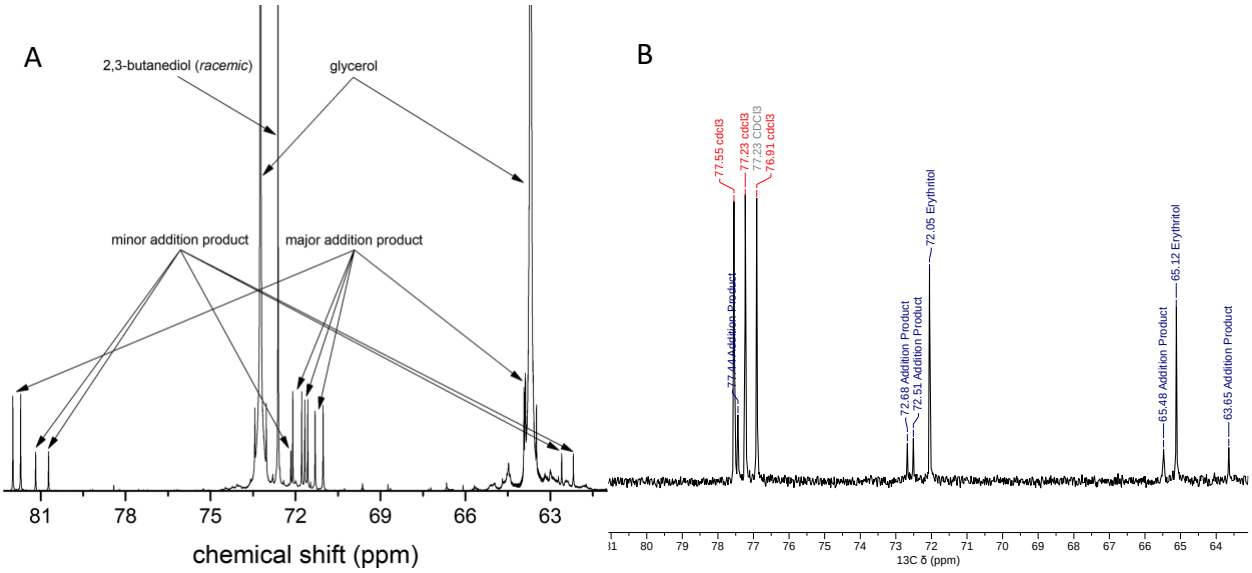

Figure 3: (A): ^{13}C NMR trace from Stropoli, et. al. for structurally similar isoprene-derived SOA compounds. [11] (B): ^{13}C NMR trace of crude dimeric product mixture, with characteristic peaks in the same range as in A.

Once the presence of dimers was confirmed, the crude product mixture was derivatized with TBDPS group to preferentially substitute at the terminal hydroxyl moieties in the reaction mixture. The derivatization was performed to add a chromophore to the compounds such that UV detection could be employed during HPLC separation. After azeotropic distillation with toluene was used to remove the majority of the pyridine, several $CuSO_4$ liquid-liquid extractions were performed, ensuring there was no characteristic color shift to a darker blue solution resulting from copper-pyridine complex formation.

The HILIC separation was performed on both derivatized and underivatized reaction mixtures. The resulting TIC, as well as the EIC for underivatized monomeric, dimeric, and trimeric species can be seen in Figure 4. The derivatized compounds were run using the same technique, with similarly resulting TIC and EICs shown in Figure 5.

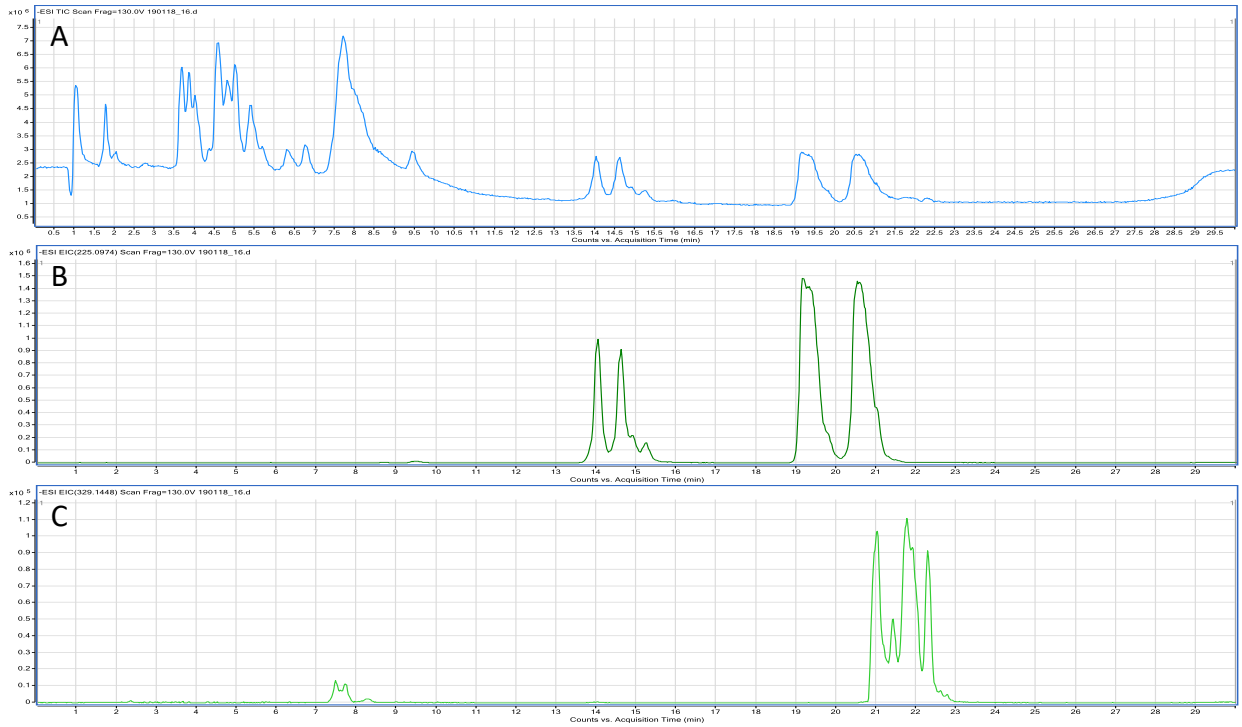

Figure 4: (A): Total Ion Chromatogram (TIC) for underivatized crude dimer product using HILIC chromatography. (B): Extracted Ion Chromatogram (EIC) for *m/z* = 225 (dimeric product). (C): EIC for *m/z* = 329 (trimeric product).

Figure 5: (A): TIC for TBDPS derivatized crude dimer product using HILIC chromatography. (B): EIC for *m/z* = 701 (bis-derivatized dimeric product). (C): EIC for *m/z* = 805 (bis-derivatized trimeric product).

After performing the HILIC method with the derivatized compounds with poor resolution, the separation was performed on a fluorophenyl-reversed phase column. The resulting TIC can be seen in Figure 6, and can be detected using a UV detector at 254 nm due to the resultant phenyl chromophore after TBDPS derivatization.

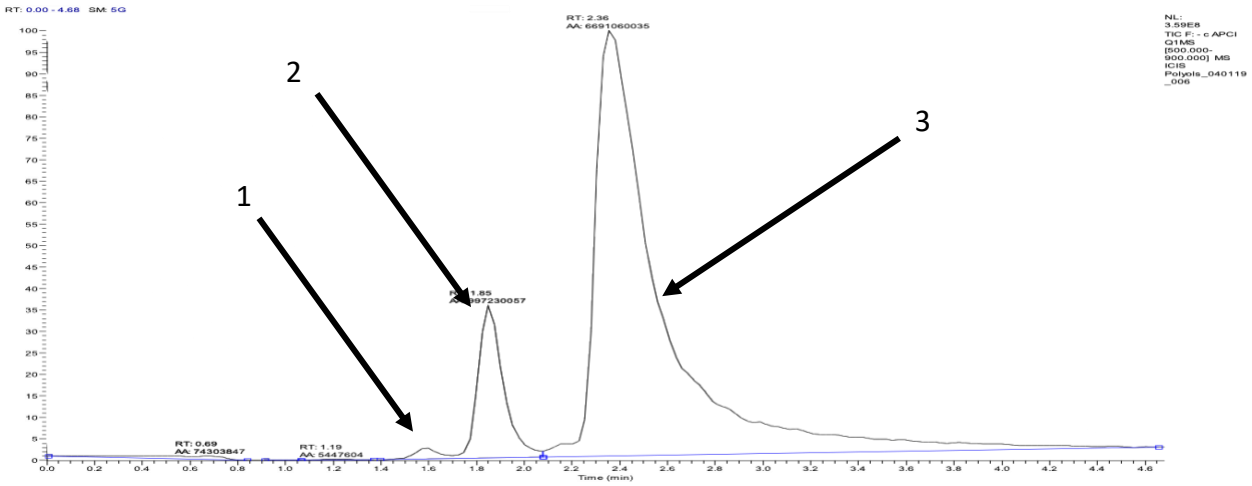

Figure 6: TIC for preliminary run with fluoro-phenyl column. Peak 1 was comprised of *m/z* = 805 (bis-derivatized trimeric) compound, peak 2 was comprised of *m/z* = 701 (bis-derivatized dimeric) compound, and peak 3 was comprised of *m/z* = 597 (bis-derivatized monomeric) compound.

Discussion:

Conversion of monomeric *meso*-erythritol was confirmed in Figures 1 and 2 by gas chromatography and ^{13}C NMR. The EIC from the GC/MS for 465, corresponding to a commonly used diagnostic ion for the TMS derivatized dimeric compound as identified by Surratt, et. al., shows a clear emergence of longer retention time peaks, as compared to the single monomeric peak seen in Figure 1A.[9] Assuming that diastereomers are not resolved by the GC, the three peaks observed can be tentatively assigned to the expected 1º – 1º, 1º – 2º and 2º – 2º coupled isomers. The characteristic NMR signals from structurally similar dimeric compounds identified in Stropoli, et. al., are seen clearly in Figure 2A, with several peaks in the 75-70 ppm range of the ^{13}C NMR spectrum.[11] Similarly shifted peaks from the dimeric product formed from the dimerization reaction with *meso*-erythritol can be seen in Figure 2B, there are several addition products seen from the ^{13}C NMR spectrum of the crude product. The ^{13}C signals at the low end of the range are predicted for the secondary O – C carbons and support the formation of 1º – 2º and/or 2º – 2º bonds, consistent with the GC/EI-MS trace. With this confirmation, chromatographic separation was first attempted on the crude product via silica stationary phase thin layer chromatography without success, as well as conventional reverse-phase liquid chromatography (data not shown).

Because UV-vis was the only detection method available for semi-preparative chromatographic separation, a chromophore was introduced to the sample by derivatizing with a *tert*-butyldiphenylsilyl protecting group (TBDPS), that can be removed via treatment with tetrabutylammonium fluoride. After the derivatization reaction was performed, a ^{1}H

NMR spectra and direct loop injection ESI-MS were used to confirm the presence of the phenyl-containing silyl protecting groups in the sample (data not shown).

The HILIC method is a recent development in LC designed to allow separation of highly polar, water soluble mixtures that elute at or near one column volume on conventional reverse phase columns. The HILIC column contains silica packing chemically bonded to polar groups, such as amide groups in the case of the BEH column used in this study.[12] With an aqueous:organic eluent, the bonded polar groups create a water-rich layer partially immobilized on the stationary phase, and analytes partition between the bulk organic eluent and the water-rich layer. Separation occurs according to relative affinity of analytes for the water layer, with a result that retention times are increased and resolution of highly polar analytes is substantially improved when compared to conventional reverse phase HPLC separation.[13] Importantly, the mobile phase is typically acetonitrile:water, so the HILIC method is compatible for interfacing with an ESI-MS source, which permitted mass calculations of the eluted peaks.

The HILIC separation proved successful when applied to the underivatized sample, showing excellent resolution in monomer, dimer, and trimer when using MS detection. Without the silyl derivation, the lack of a chromophore precluded observation of a UV trace at analyte concentrations compatible with column capacity, leading to difficulties collecting fractions via UV detection for further characterization. In efforts to be able to identify these peaks with UV detection, the HILIC method was performed with the derivatized products. However, the resulting EIC for monomer, dimer, and trimer showed very short column retention times corresponding closely to the time to pass one column volume. Because the compounds were not retained on the BEH Amide column in HILIC mode, fluoro-phenyl reversed phase methods were explored with the UV-detectable silyl derivatives, as the derivatized groups provided several phenyl moieties that could bind more readily to the stationary phase.

The resulting TIC for the derivatized products showed promising peak resolution, with several sharp, high intensity peaks using a simple, isocratic method. Upon further evaluation of the mass spectra collected from each of these peaks, they indicated successful resolution of monomeric, dimeric, and trimeric components of the overall reaction mixture. These peaks can also be detected without the use of a mass spectrometer, as the TBDPS protecting groups elicit a strong absorbance response at 254 nm with conventional UV detection, allowing these compounds to be collected *en masse* with isolated monomer, dimer, and trimer.

Conclusion:

Synthesis of dimeric compounds for use as surrogate standards in isoprene-derived SOA has been confirmed via ^{13}C NMR and mass spectrometry. Separation of dimeric oligomers for quantitation of atmospheric SOA in field samples appears promising via the HILIC method, however, well characterized isomeric compounds have yet to be isolated. These compounds already have an application as surrogate standards for extracts from isolated aerosol particulates collected on filters using the HILIC method, but cannot yet be employed for real-time quantification until complete isolation from monomeric and trimeric isomers has been accomplished. The most attractive method for analysis at present would be HILIC separation using an evaporative light-scattering or refractive

index detector for peak detection. With improvements to the chromatographic methods and ionization techniques used to analyze the separation, isolating and characterizing these compounds appears to be possible based on well-resolved peaks detected by mass spectrometry.

Once these compounds can be isolated with high fidelity, both ^{1}H and ^{13}C-NMR characterization can be performed, with extension to 2D-NMR studies for detailed structural characterization. Once a robust protocol is designed for synthesis and isolation of these compounds, the process can be further applied for use with 2-methyl erythritol as a starting material, to produce isolated compounds that are identical to those found in the atmosphere. With isolated compounds, extended studies into the health effects of these compounds and resulting cellular stresses can be analyzed by studying exposure to cardiovascular cells *in vitro*, to further understand the health risk that these compounds pose to humans.

Acknowledgements:

Dr. Avram Gold
Dr. Jason Surratt
Dr. Zhenfa Zhang
Dr. Wanda Bodnar
Leonard Collins
Peter Cable
Tianqu Cui
Yuzhi Chen
Dr. Erik Alexanian (Honors Committee Chair)
Dr. Joshua Beaver (Honors Committee Member)

References:

(1) Budisulistiorini, S. H.; Baumann, K.; Edgerton, E. S.; Bairai, S. T.; Mueller, S.; Shaw, S. L.; Knipping, E. M.; Gold, A.; Surratt, J. D. *Atmos. Chem. Phys.* **2016**, *16* (8), 5171–5189.

(2) Guenther, A.; Karl, T.; Harley, P.; Wiedinmyer, C.; Palmer, P. I.; Geron, C. *Atmos. Chem. Phys. Discuss.* **2006**, *6* (1), 107–173.

(3) Carlton, A. G.; Wiedinmyer, C.; Kroll, J. H. *Atmos. Chem. Phys.* **2009**, *9* (14), 4987–5005.

(4) Guenther, A.; Hewitt, C. N.; Erickson, D.; Fall, R.; Geron, C.; Graedel, T.; Harley, P.; Klinger, L.; Lerdau, M.; McKay, W. A.; Pierce, T.; Scholes, B.; Steinbrecher, R.; Tallamraju, R.; Taylor, J.; Zimmerman, P. *J. Geophys. Res.* **1995**, *100* (D5), 8873.

(5) Haywood, J.; Boucher, O. *Rev. Geophys.* **2000**, *38* (4), 513–543.

(6) Pope III, C. A.; Dockery, D. W. *J. Air Waste Manag. Assoc.* **2006**, *56* (6), 709–742.

(7) Lin, Y. H.; Budisulistiorini, S. H.; Chu, K.; Siejack, R. A.; Zhang, H.; Riva, M.; Zhang, Z.; Gold, A.; Kautzman, K. E.; Surratt, J. D. *Environ. Sci. Technol.* **2014**, *48* (20), 12012–12021.

(8) Guerrero-Urbaneja, P.; García-Sancho, C.; Moreno-Tost, R.; Mérida-Robles, J.; Santamaría-González, J.; Jiménez-López, A.; Maireles-Torres, P. *Appl. Catal. A Gen.* **2014**, *470*, 199–207.

(9) Surratt, J. D.; Chan, A. W. H.; Eddingsaas, N. C.; Chan, M.; Loza, C. L.; Kwan, A. J.; Hersey, S. P.; Flagan, R. C.; Wennberg, P. O.; Seinfeld, J. H. *PNAS* **2009**, *107* (15), 6640–6645.

(10) Cui, T.; Zeng, Z.; dos Santos, E. O.; Zhang, Z.; Chen, Y.; Zhang, Y.; Rose, C. A.; Budisulistiorini, S. H.; Collins, L. B.; Bodnar, W. M.; Souza, R. A. F. De; Martin, S. T.; Machado, C. M. D.; Turpin, B. J.; Gold, A.; Ault, P.; Surratt, J. D. *Environ. Sci. Process. Impacts* **2018**.

(11) Stropoli, S. J.; Miner, C. R.; Hill, D. R.; Elrod, M. J. *Environ. Sci. Technol.* **2018**, *53*, 176–184.

(12) Pavel, J. *J. Sep. Sci.* **2008**, *31* (9), 1421–1437.

(13) Hemström, P.; Irgum, K. *J. Sep. Sci.* **2006**, *29* (12), 1784–1821.